

Transient Shear Flow Behavior of Dilute Solutions of Side-Chain Liquid-Crystalline Polysiloxanes in 4,4'-(*n*-Pentyloxy)cyanobiphenyl

Ning Yao and Alex M. Jamieson*

Department of Macromolecular Science, Case Western Reserve University, Cleveland, Ohio 44106-7202

Received February 2, 1998; Revised Manuscript Received May 18, 1998

ABSTRACT: The transient stress response of homeotropic monodomains of dilute nematic solutions of side-chain liquid-crystalline polysiloxanes (LCPs) in 4,4'-(*n*-pentyloxy)cyanobiphenyl (5OCB) is investigated. In contrast to the flow-aligning behavior of 5OCB, strong stress oscillations are observed for the dilute LCP solutions, characteristic of flow-tumbling behavior. The dependence of the oscillation periodicity on LCP concentration and LCP structure (molecular weight and spacer length) is presented. From analysis of the stress transients, the Leslie viscosity coefficients, α_2 and α_3 , are calculated. For all LCP structures, the increment $\delta\alpha_2$ on dissolution of LCP is negative, whereas the increment $\delta\alpha_3$ is positive. The magnitude and signs of these viscosity increments are strictly inconsistent with earlier electrorheological measurements of the Miesowicz viscosity increments, $\delta\eta_b$ and $\delta\eta_c$, of these solutions, using as a guide a hydrodynamic model that computes the contribution of the chains to viscous dissipation in a simple shear flow. We propose that an additional dissipation mechanism should be considered, which derives from the presence of an elastic torque between director rotation and LCP orientation. Corresponding modification of the theory leads to improved agreement with experiment.

Introduction

When a nematic monodomain is subjected to a shear flow, the orientational response of the nematic director is determined principally by two of the six Leslie viscosity coefficients, viz., α_2 and α_3 .^{1,2} The nematic shows flow-aligning behavior; i.e., the director aligns at a characteristic angle close to the flow direction, when the product $\alpha_2\alpha_3$ is positive. On the other hand, flow-tumbling behavior is observed; i.e., the director is forced to rotate continuously by hydrodynamic torques, if $\alpha_2\alpha_3$ is negative. Since α_2 is generally negative, the sign of α_3 determines the orientational response of the nematic: flow-aligning when $\alpha_3 < 0$ and flow-tumbling when $\alpha_3 > 0$.

According to Ericksen's³ transversely isotropic fluid (TIF) theory, when the director is initially aligned perpendicular to the flow, and parallel to the velocity gradient, as shown in Scheme 1, a simple stress overshoot is predicted for a flow-aligning nematic in start-up shear flow, whereas a stress oscillation should be observed for a tumbling nematic. Specifically, Ericksen's TIF theory predicts that the apparent viscosity η_{app} varies as^{4,5}

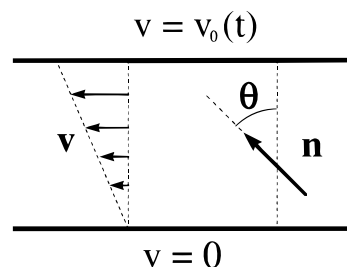
$$\tau_{xy} = \dot{\gamma}\eta_{app} = \dot{\gamma} \left\{ \left[\alpha_1 + \frac{(\alpha_3 + \alpha_2)^2}{\alpha_3 - \alpha_2} \right] \sin^2 \theta \cos^2 \theta + \eta_b - \frac{\alpha_3^2}{\alpha_3 - \alpha_2} \right\} \quad (1)$$

and the director evolution equation is

$$\frac{\partial \theta}{\partial t} = \frac{(\alpha_3 \sin^2 \theta - \alpha_2 \cos^2 \theta)}{\alpha_3 - \alpha_2} \dot{\gamma} \quad (2)$$

where $\dot{\gamma}$ is the shear rate, α_1 , α_2 , and α_3 are the first, second, and third Leslie viscosity coefficients, $\eta_b = (\alpha_3 + \alpha_4 + \alpha_6)/2$ is one of the Miesowicz viscosities. The

Scheme 1. Homeotropic Monodomain Subjected to a Shear Flow



value of θ , the angle of the director relative to the shear gradient direction, as shown in Scheme 1, is given by

$$\tan \theta = \left(\frac{-\alpha_2}{\alpha_3} \right)^{0.5} \tan \left[\frac{(-\alpha_2\alpha_3)^{0.5}}{\alpha_3 - \alpha_2} \gamma \right] \quad \text{for } \alpha_3 > 0 \quad (3)$$

and

$$\tan \theta = \left(\frac{\alpha_2}{\alpha_3} \right)^{0.5} \tanh \left[\frac{(\alpha_2\alpha_3)^{0.5}}{\alpha_3 - \alpha_2} \gamma \right] \quad \text{for } \alpha_3 < 0 \quad (4)$$

As evident from eqs 1, 3, and 4, the apparent viscosity η_{app} is a function of the director rotation angle, which depends on shear strain γ . A single maximum is predicted at $\theta = \pi/4$ for a flow-aligning nematic, while for a tumbling nematic, a series of maxima occur at $\theta = m\pi/4$ ($m = \text{odd}$), and a series of minima at $\theta = n\pi/2$ ($n = 0, 1, 2, 3, \dots$).⁶ Experimentally, the rheological behavior predicted by eqs 1–4 for flow-aligning and tumbling low molar mass nematics (LMMNs) has been observed,^{4,5,7} with the exception that, for tumbling LMMNs, the oscillations in η_{app} are damped with increasing strain. The latter behavior appears to be due to nucleation of out-of-plane director orientations.^{8–12}

When a small amount of liquid-crystalline polymer (LCP) is dissolved in an LMMN, a dramatic change in flow behavior may occur.^{4,7,13,14} Dissolution of a side-

* To whom all correspondence should be addressed.

chain LCP in a flow-aligning LMMN was observed to cause a transition to flow-tumbling behavior;^{4,7,14} dissolution of a main-chain LCP in a tumbling LMMN was found to produce a flow-aligning solution.⁴ These observations are qualitatively consistent with a hydrodynamic model by Brochard,¹⁵ which describes the viscosity increments due to dissolution of an LCP in an LMMN in terms of several microscopic parameters such as $R_{||}$, R_{\perp} (the rms end-to-end distance of the polymer chain perpendicular and parallel to the director), and τ_r , the conformational relaxation time of the LCP:

$$\delta\gamma_1 = \frac{(R_{\perp}^2 - R_{||}^2)^2}{R_{\perp}^2 R_{||}^2} \left(\frac{ckT}{N} \right) \tau_r \quad (5)$$

$$\delta\gamma_2 = \frac{R_{\perp}^4 - R_{||}^4}{R_{\perp}^2 R_{||}^2} \left(\frac{ckT}{N} \right) \tau_r \quad (6)$$

where γ_1 is the twist viscosity, characterizing the hydrodynamic torque on the director from the rotational part of the flow, γ_2 characterizes the torque from the irrotational part of the flow, c is the LCP concentration, k is Boltzmann's constant, T is the absolute temperature, and N is the molecular mass of the LCP. Application of the relations $\alpha_2 = (\gamma_2 - \gamma_1)/2$ and $\alpha_3 = (\gamma_2 + \gamma_1)/2$ to eqs 5 and 6 yields^{4,5}

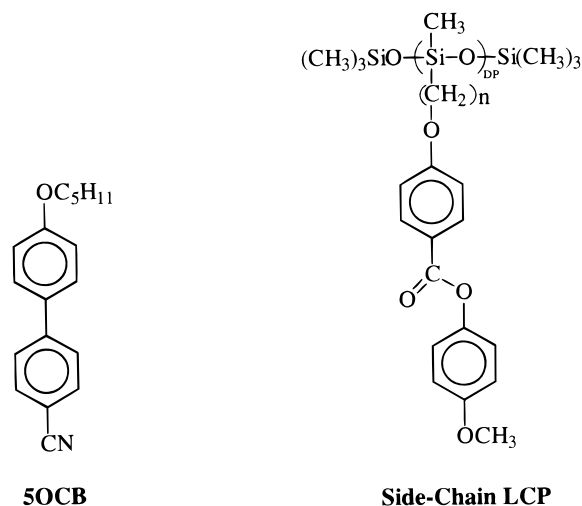
$$\delta\alpha_2 = \frac{R_{\perp}^2 - R_{||}^2}{R_{\perp}^2} \left(\frac{ckT}{N} \right) \tau_r \quad (7)$$

$$\delta\alpha_3 = \frac{R_{\perp}^2 - R_{||}^2}{R_{||}^2} \left(\frac{ckT}{N} \right) \tau_r \quad (8)$$

Equations 7 and 8 indicate that the magnitude and sign of $\delta\alpha_2$ and $\delta\alpha_3$ are dependent on the anisotropy ratio $R_{||}/R_{\perp}$. Specifically, both $\delta\alpha_2$ and $\delta\alpha_3$ are predicted to be negative when $R_{||} > R_{\perp}$. Such a case is expected for main-chain LCP solutions. Thus the Brochard model predicts, in agreement with observation, that addition of a main-chain LCP, which has a prolate conformation, to a tumbling nematic will produce a flow-aligning solution ($\delta\alpha_3 < 0$). When $R_{\perp} > R_{||}$, the model predicts $\delta\alpha_2$ and $\delta\alpha_3$ are both positive. A positive $\delta\alpha_3$, when α_2 remains negative, indicates that addition of a side-chain LCP, which has an oblate conformation, to a flow-aligning LMMN produces a flow-tumbling solution, as indeed observed experimentally. A discrepancy was observed,⁴ however, when the experimental data were analyzed in terms of Ericksen's TIF theory (eqs 1–4) to extract values of α_2 and α_3 . It was found that, while experimental values of $\delta\alpha_2$ and $\delta\alpha_3$ for the main-chain LCP solution were each negative, in agreement with the Brochard model, for the side-chain LCP solution, $\delta\alpha_3$ was positive but $\delta\alpha_2$ was negative, in disagreement with the model.

In this paper, the transient shear flow behavior of dilute solutions of side-chain liquid-crystalline polysiloxanes dissolved in 4,4'-(*n*-pentyloxy)cyanobiphenyl (5OCB) is studied. The dependence on LCP concentration, molecular weight, and spacer length is examined. Whereas pure 5OCB shows flow-aligning behavior, the side-chain LCP solutions generally show flow-tumbling behavior. This observation implies, via the Brochard model, that the chain conformation is oblate and con-

Chart 1. Structures of 5OCB and the Side-Chain LCP



tradicts an earlier deduction, that the LCP conformation is prolate, based on electrorheological (ER) measurements¹⁶ of the Miesowicz viscosity increments $\delta\eta_b$ and $\delta\eta_c$. The latter data were interpreted, again via the Brochard model, using the equation

$$\frac{R_{||}^4}{R_{\perp}^4} = \frac{\delta\eta_c}{\delta\eta_b} \quad (9)$$

Employing the procedure established previously,⁴ the values of the second and third Leslie coefficients, viz., α_2 and α_3 , of the LCP/5OCB solutions are calculated for all molecular weights and spacer lengths. We find that the $\delta\alpha_2$ values are negative whereas $\delta\alpha_3$ are positive, confirming that the flow behavior is only partially consistent with the Brochard model. To resolve these discrepancies, we propose that an additional viscous dissipation mechanism exists because of an elastic coupling between director rotation and chain orientation.

Experimental Section

5OCB ($T_{N-I} = 67^\circ\text{C}$) was purchased from Aldrich Chemical Co. and used as received. The side-chain LCPs ($DP = 45, 127, 198$; $n = 3, 5, 11$) were synthesized via the hydrosilation reaction between poly(methylhydrosiloxane) and appropriate olefins.¹⁶ The structures of 5OCB and the side-chain LCP are shown in Chart 1. L- α -Lecithin was purchased from Sigma Chemical Co. and used as a 0.5 wt % solution in ethanol.

Transient shear flow experiments were performed on a Rheometrics fluids rheometer with stainless steel cone-and-plate geometry (cone angle = 0.02 rad and cone radius = 25 mm) at shear rate = 32 s^{-1} using previous methodology.^{4,5,7} The inner surfaces of the cone and the plate were treated with a 0.5 wt % ethanol solution of L- α -lecithin to achieve surface anchoring for homeotropic alignment. The sample temperature was controlled accurate to 0.1°C . Each measurement was made 15 min after the sample was loaded or subjected to a prior test.

Results

Stress Transients of Dilute Solutions of the Side-Chain LCPs in 5OCB. 5OCB is a flow-aligning nematic and a single stress overshoot peak appears over the entire nematic regime (Figure 1). In contrast, periodic stress oscillations with the characteristic double peak feature are observed when the side-chain LCPs are dissolved in 5OCB, as demonstrated in

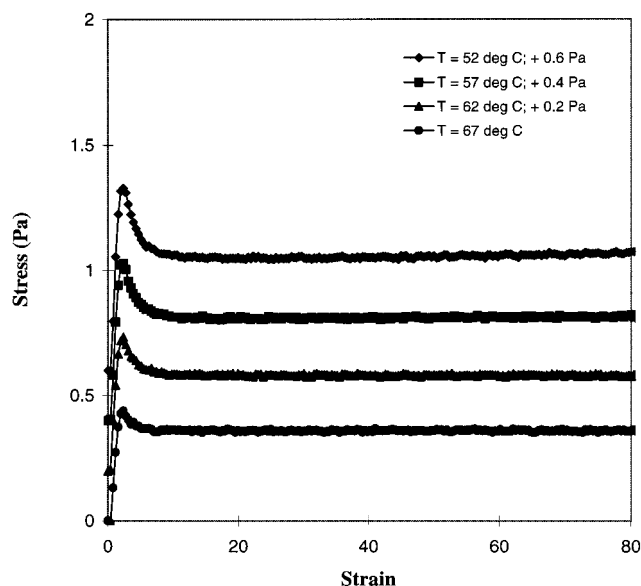


Figure 1. Stress transients of 5OCB at different temperatures. The curves are shifted by certain stress units to avoid overlapping.

Table 1. Periodicity (Strain Unit) of Stress Oscillations of 5OCB Solutions of the Side-Chain Liquid-Crystalline Polysiloxanes

DP	<i>n</i>	<i>c</i> (g/mL)	52 °C	57 °C	62 °C	67 °C
198	3	0.005	35.8	52.2		
198	3	0.01	17.2	17.7	19.7	50
198	3	0.02	10.6	10.3	10.1	10.0
198	3	0.03	8.8	8.5	8.2	8.0
127	3	0.005	40.2	80		
127	3	0.01	19.2	20.0	24.5	90
127	3	0.02	12.2	11.9	11.7	12.1
127	3	0.03	9.6	9.3	9.1	9.0
45	3	0.005	125			
45	3	0.01	34.5	64		
45	3	0.02	17.7	18.4	21.2	85
45	3	0.03	13.2	13.3	13.6	15.5
45	5	0.005	115			
45	5	0.01	54.0	100		
45	5	0.02	22.9	25.0	39.5	
45	5	0.03	16.7	17.2	18.8	30.5
45	11	0.005	110			
45	11	0.01	71.5	80		
45	11	0.02	27.2	34.5	75	
45	11	0.03	19.6	21.0	27.6	

Figures 2–5. These observations are consistent with the previous observations of Gu et al.^{4,7} carried out on a different side-chain LCP in a different flow-aligning nematic (5CB). From the transient shear flow experiments, the strain periodicity was measured with good accuracy and the results are listed in Table 1. It can be seen from Figure 2 and Table 1 that the strain periodicity increases as the concentration of the LCP/5OCB solutions decreases. The temperature dependence of the strain periodicity is complicated. When the molecular weight of the side-chain LCPs is low, i.e., DP = 45, the periodicity increases with an increase of temperature at all four concentrations. However, when the molecular weight is high, i.e., DP = 127 or 198, the periodicity increases with temperature when the concentration is relatively low and decreases with temperature when the concentration is relatively high (Figure 3). At a fixed temperature or concentration, the periodicity increases as the molecular weight decreases (Figure 4) or spacer length increases (Figure 5). These results indicate that the rheological behavior of the

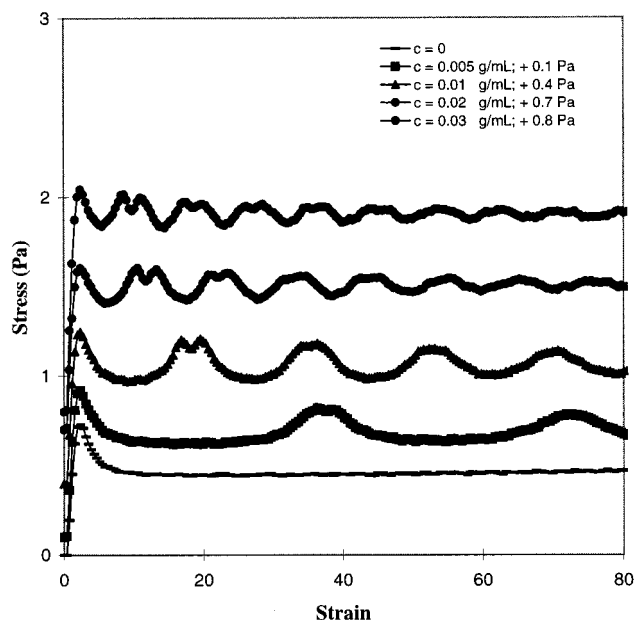


Figure 2. Stress transients of 5OCB solutions of the side-chain LCP with different concentrations (DP = 198, *n* = 3, *T* = 52 °C). The curves are shifted by certain stress units to avoid overlapping.

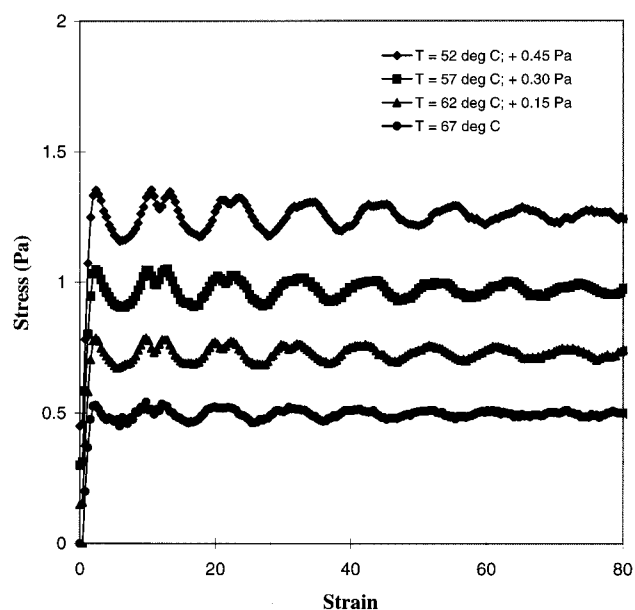


Figure 3. Stress transients of 5OCB solutions of the side-chain LCP at different temperatures (DP = 198, *n* = 3, *c* = 0.02 g/mL). The curves are shifted by certain stress units to avoid overlapping.

nematic solutions is very sensitive to the molecular structure of the side-chain LCPs.

It is well-known that nonspherical conformations are typical for an LCP in a nematic solvent.^{2,16–23} According to the Brochard model,¹⁵ as evident in eqs 7 and 8, factors such as temperature, molecular weight, and spacer length, which can change the anisotropy ratio of an LCP in the nematic solvent, will influence the strain periodicity of the LCP solution, as indeed observed in Figures 2–5 and Table 1. Also, we note, in agreement with Gu et al.,^{4,7} that while the periodicity remains constant for a given solution, the oscillation amplitude invariably dampens with an increase of strain. This behavior appears to arise from out-of-plane motion of the director at large strain.^{8–12} In theoretical

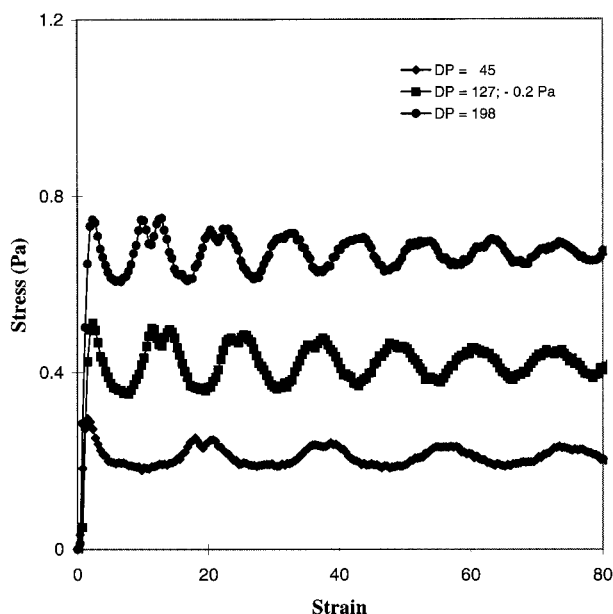


Figure 4. Stress transients of 5OCB solutions of the side-chain LCPs with different DP ($n = 3$, $T = 57^\circ\text{C}$, $c = 0.02\text{ g/mL}$). The middle curve is shifted by -0.2 Pa to avoid overlapping.

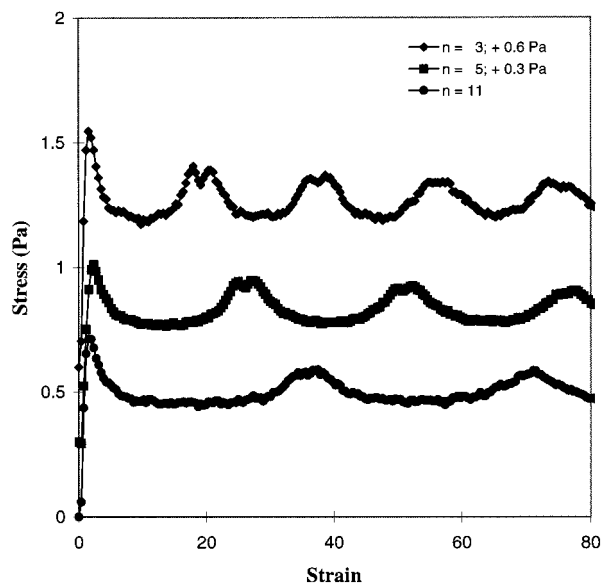
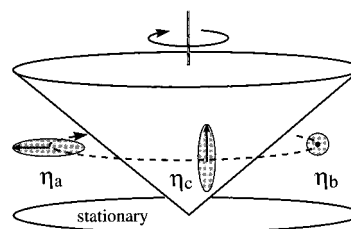


Figure 5. Stress transients of 5OCB solutions of the side-chain LCPs with different spacer lengths ($\text{DP} = 45$, $T = 57^\circ\text{C}$, $c = 0.02\text{ g/mL}$). The curves are shifted by certain stress units to avoid overlapping.

analysis using Ericksen's TIF theory, Burghardt¹² found that, on imposing an increasing degree of tilt toward the velocity direction, a decrease is predicted in the amplitude of the transient stress oscillation, and a diminishing of the doublet feature, but no change in oscillation periodicity. Also, in 3D simulation of planar shear flow using Ericksen's TIF theory, Rey et al.^{8,9} found that the stress oscillations dampen because of nucleation of out-of-plane defects. Experimentally, Mather et al.¹⁰ have demonstrated a correlation between damping of the oscillations in the transient stress and the appearance of twist walls in rotating disk geometry.

Quantitative Analysis of the Stress Transients of Nematics. According to Ericksen's TIF theory (eqs 1–4), the apparent viscosity of a homeotropic nematic monodomain subjected to a shear flow is a function of the Leslie coefficients, α_1 , α_2 , and α_3 and the Miesowicz

Scheme 2. Three Miesowicz Viscosities



viscosity η_b . On the other hand, the Brochard model describes the viscosity increments of α_2 and α_3 due to dissolution of an LCP in an LMMN in terms of several microscopic parameters such as $R_{||}$, R_{\perp} , and τ_r (eqs 7 and 8). To gain a better understanding of the flow behavior of nematics, a quantitative analysis of α_2 and α_3 is needed. This can be achieved via a numerical analysis of the stress transients, as established previously.⁴

Scheme 2 schematically illustrates, for cone-and-plate geometry, that three orientations of a nematic director in a shear flow are important. The viscosities when the director is fixed in one of these three orientations are commonly called the Miesowicz viscosities η_a , η_b , and η_c . Recently, we have described measurements of the η_b and η_c by ER observations.^{16,21–23} Our results indicate that for both flow-aligning and tumbling nematics, η_c can be obtained with high precision. The Miesowicz viscosities can be expressed as linear combinations of the Leslie coefficients:²

$$\eta_a = \frac{1}{2}\alpha_4 \quad (10)$$

$$\eta_b = \frac{1}{2}(\alpha_3 + \alpha_4 + \alpha_6) \quad (11)$$

$$\eta_c = \frac{1}{2}(-\alpha_2 + \alpha_4 + \alpha_5) \quad (12)$$

Only five of the six Leslie coefficients are independent because of the Parodi relation:²⁴

$$\alpha_2 + \alpha_3 = \alpha_6 - \alpha_5 \quad (13)$$

Application of eq 13 to eqs 11 and 12 gives

$$\alpha_2 + \alpha_3 = \eta_b - \eta_c \quad (14)$$

Gu et al.^{4,5} have previously demonstrated that values of α_2 and α_3 can be obtained by fitting the initial stress transients to eqs 1–4 provided an independent viscosity measurement is available. Here we determine α_2 and α_3 from the stress transients, as shown in Figures 2–5, using the procedure established by Gu et al.^{4,5} with slight modification. First we rewrite eq 1 using eq 14:

$$\eta_{\text{app}} = \left[\alpha_1 + \frac{(\alpha_3 + \alpha_2)^2}{\alpha_3 - \alpha_2} \right] \sin^2 \theta \cos^2 \theta + \eta_c - \frac{\alpha_2^2}{\alpha_3 - \alpha_2} \quad (15)$$

Also, following Gu et al.,^{4,5} we add a term, $\delta\gamma$, to eqs 3 and 4 to correct for a strain delay of the stress transients resulting from mechanical inertia:

$$\tan \theta = \left(\frac{-\alpha_2}{\alpha_3} \right)^{0.5} \tan \left[\frac{(-\alpha_2 \alpha_3)^{0.5}}{\alpha_3 - \alpha_2} (\gamma + \delta \gamma) \right] \quad \text{for} \quad \alpha_3 > 0 \quad (16)$$

As noted by Gu et al.,⁴ an unambiguous solution can be obtained only when there are three independent parameters in eqs 1–4. To reduce the number of independent parameters in eqs 15 and 16 to three, we use values of the Miesowicz viscosity, η_c , determined from ER experiments. Moreover, the following equation is applied:²⁵

$$\gamma_p = \frac{\pi(1 + \delta^2)}{\delta} \quad (17)$$

where γ_p is the strain periodicity of the stress oscillations, $\delta = (-\alpha_3/\alpha_2)^{0.5}$. Shown in Figure 6 is the comparison between a measured stress transient (DP = 198, $n = 3$, $T = 52^\circ\text{C}$, $c = 0.01\text{ g/mL}$) and a calculated stress transient via eq 15. A good fit is evident at low strains. Using this fitting procedure, the values of α_2 and α_3 of the LCP/5OCB solutions were determined. The viscosity increments, $\delta\alpha_2$ and $\delta\alpha_3$, of the LCP/5OCB solutions relative to 5OCB²⁰ are shown in Figures 7–10. It can be seen from Figures 7–10 that $\delta\alpha_3$ increases with LCP concentration, whereas $\delta\alpha_2$ decreases with LCP concentration. This result confirms earlier observations of Gu et al.^{4,7} and is only partially consistent with the prediction of the Brochard model as embodied in eqs 7 and 8. The values of $\delta\alpha_2$ and $\delta\alpha_3$ approach each other with increasing temperature. Moreover, $\delta\alpha_3$ shows an increasing trend with an increase in molecular weight whereas $\delta\alpha_2$ appears independent of molecular weight. The latter result is consistent with previous measurements of the molecular weight dependence of $\delta\eta_c$. Figure 10 shows that $\delta\alpha_2$ and $\delta\alpha_3$ each show a decreasing trend with an increase of spacer length. In all cases, $\delta\alpha_2$ is negative whereas $\delta\alpha_3$ is positive.

Discussion

As the stress transient experiments show, the dissolution of a side-chain LCP in a flow-aligning LMMN produces a solution that exhibits flow-tumbling behavior, as predicted by the Brochard model, if the chain conformation is oblate. Such an interpretation is, however, strictly inconsistent with our earlier ER measurements, which led to the conclusion, via eq 9, that the chain is prolate. According to Ericksen's TIF theory, a flow-aligning nematic has a negative α_3 and a tumbling nematic has a positive α_3 , provided that α_2 is negative. Thus, the increment of α_3 , $\delta\alpha_3$, must be positive if flow-tumbling behavior is observed for the solution of an LCP dissolved in a flow-aligning LMMN. Since, from eq 14, it follows that

$$\delta\alpha_2 + \delta\alpha_3 = \delta\eta_b - \delta\eta_c \quad (18)$$

it is evident, in principle, that $\delta\alpha_2$ can be either positive or negative, depending on the relative values of $\delta\eta_b$ and $\delta\eta_c$. Experimentally, we observe negative $\delta\alpha_2$ and positive $\delta\alpha_3$ for all side-chain LCP solutions in 5OCB. However, the Brochard model,¹⁵ embodied in eqs 7 and 8 predicts that $\delta\alpha_2$ and $\delta\alpha_3$ should always have the same sign. The origin of these discrepancies is unclear. However, examination of the results suggests that there is an additional contribution to the rotational viscosities

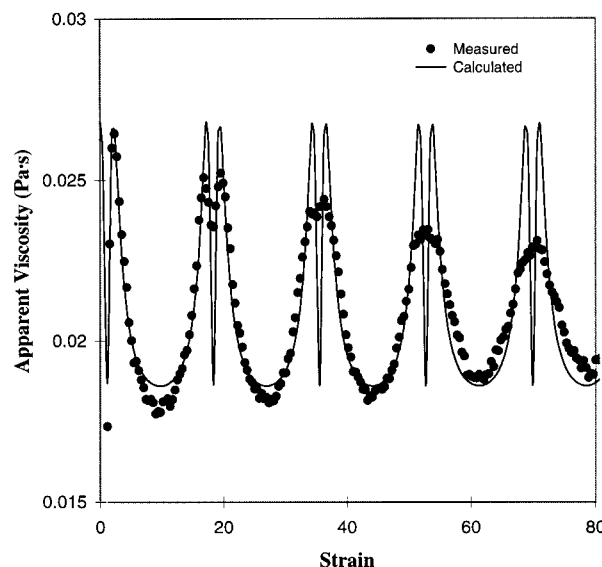


Figure 6. Theoretical fits (eqs 1–4) to the stress transient of a 5OCB solution of the side-chain LCP (DP = 198, $n = 3$, $T = 52^\circ\text{C}$, $c = 0.01\text{ g/mL}$).

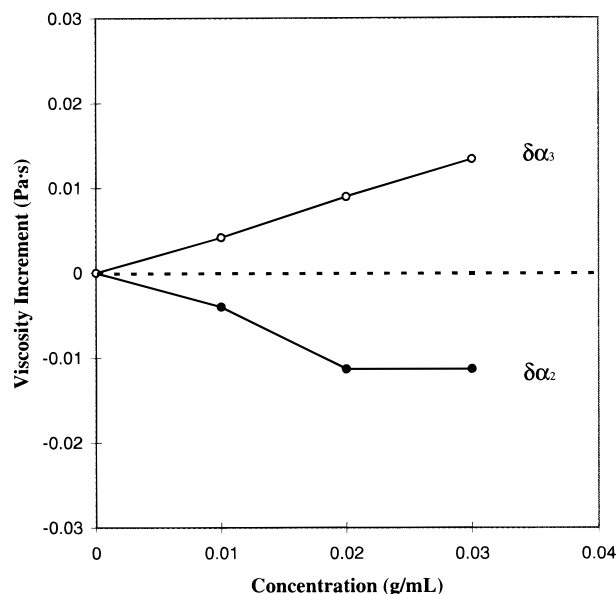


Figure 7. Concentration dependence of $\delta\alpha_2$ and $\delta\alpha_3$ of 5OCB solutions of the side-chain LCP (DP = 198, $n = 3$, $T = 52^\circ\text{C}$).

$\delta\gamma_1$, $\delta\alpha_2$, and $\delta\alpha_3$. The analysis of Brochard computes the contribution of the LCP chains to the hydrodynamic torque Γ on the director \vec{n} in a nematic medium:

$$\Gamma = \vec{n} \times \left[\gamma_1 \left(\frac{d\vec{n}}{dt} \cdot \vec{n} \right) + \gamma_2 \vec{A} \cdot \vec{n} \right] \quad (19)$$

where $\omega = 1/2 \nabla \times \vec{v}$ is the antisymmetric velocity gradient tensor, and A is the symmetric velocity gradient tensor, $A_{\alpha\beta} = 1/2(\partial_\alpha v_\beta + \partial_\beta v_\alpha)$. Brochard computed the contributions to Γ_y , the torque about the vorticity axis, from flows in the xz plane. Phenomenologically, we propose that in the absence of a viscous flow, an additional contribution to the torque can arise because of an elastic coupling between director rotation and the orientation of the LCP chain.²⁶ It is envisaged that this torque contribution $\delta\Gamma_y^{\text{el}}$ produces viscous dissipation by causing rotation of the chain about the vorticity axis. The chain rotation is opposed by a frictional torque $v\xi$, where ξ is the rotary frictional coefficient and $v = d\vec{n}/dt$

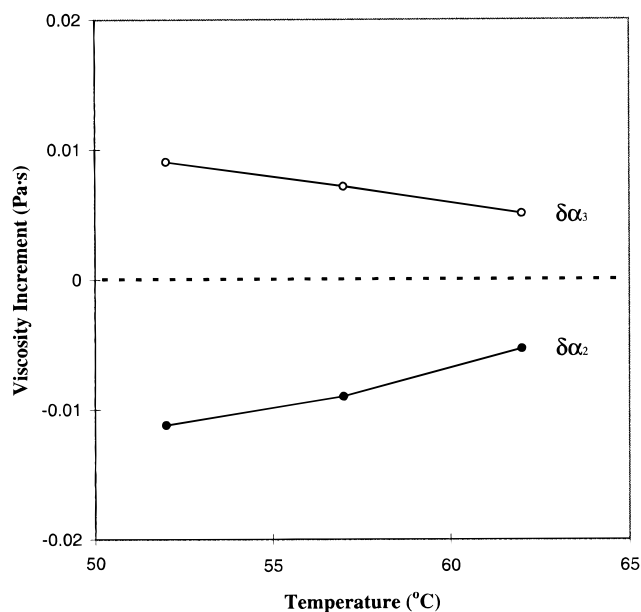


Figure 8. Temperature dependence of $\delta\alpha_2$ and $\delta\alpha_3$ of 5OCB solutions of the side-chain LCP (DP = 198, $n = 3$, $c = 0.02$ g/mL).

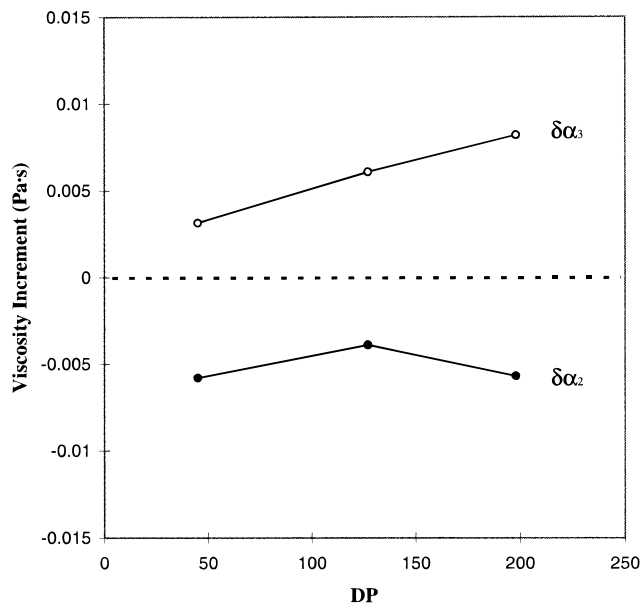


Figure 9. DP dependence of $\delta\alpha_2$ and $\delta\alpha_3$ of 5OCB solutions of the side-chain LCPs ($n = 3$, $T = 62$ °C, $c = 0.03$ g/mL).

is the rate of director rotation. In steady state, we have

$$\delta\Gamma_y^{\text{el}} = \delta\gamma_1^{\text{el}}v = \left(\frac{c}{N}\right)v\xi = \left(\frac{c}{N}\right)vkT\tau_{\text{rot}} \quad (20)$$

where $\delta\gamma_1^{\text{el}}$ is the additional contribution to the rotational viscosity, and $\tau_{\text{rot}} = kT/\xi$ is the rotational relaxation time. Thus

$$\delta\gamma_1^{\text{el}} = \left(\frac{ckT}{N}\right)\tau_{\text{rot}} \quad (21)$$

For quasi-spherical particles, we may equate $\tau_{\text{rot}} = \tau_r$ and obtain a modified version of Brochard's equation for $\delta\gamma_1$:

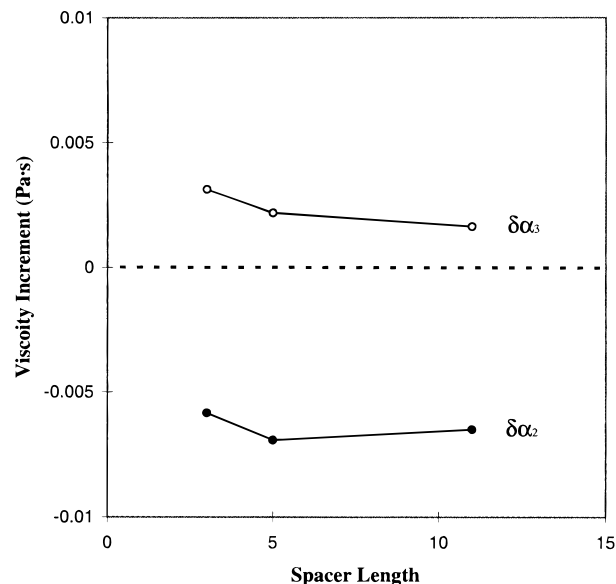


Figure 10. Spacer length dependence of $\delta\alpha_2$ and $\delta\alpha_3$ of 5OCB solutions of the side-chain LCPs (DP = 45, $T = 62$ °C, $c = 0.03$ g/mL).

$$\delta\gamma_1 = \left[\frac{(R_{\perp}^2 - R_{\parallel}^2)^2}{R_{\perp}^2 R_{\parallel}^2} + 1 \right] \left(\frac{ckT}{N} \right) \tau_r \quad (22)$$

Since $\alpha_2 = (\gamma_2 - \gamma_1)/2$ and $\alpha_3 = (\gamma_2 + \gamma_1)/2$, it follows that

$$\delta\alpha_2 = \left(\frac{1}{2} - \frac{R_{\parallel}^2}{R_{\perp}^2} \right) \left(\frac{ckT}{N} \right) \tau_r \quad (23)$$

$$\delta\alpha_3 = \left(\frac{R_{\perp}^2}{R_{\parallel}^2} - \frac{1}{2} \right) \left(\frac{ckT}{N} \right) \tau_r \quad (24)$$

As evident from eqs 23 and 24, $\delta\alpha_2$ and $\delta\alpha_3$ are still dependent on the anisotropy ratio R_{\parallel}/R_{\perp} but may now have different signs.

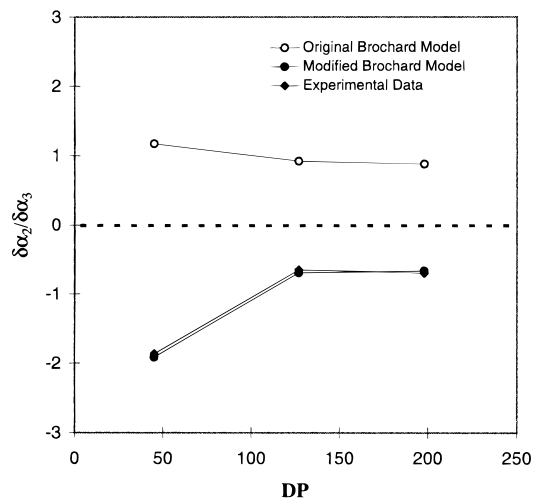
For dilute solutions of main-chain LCPs dissolved in LMMNs, $\delta\eta_c$ is normally much greater than $\delta\eta_b$, which means $R_{\parallel}^2/R_{\perp}^2$ is much greater than 2. According to eqs 23 and 24, both $\delta\alpha_3$ and $\delta\alpha_2$ will therefore be negative which agrees with experimental observations.⁴ Thus, eqs 23 and 24, remain consistent with our experimental observation that, when a main-chain LCP is dissolved in a tumbling LMMN, the flow-tumbling behavior is suppressed and flow-aligning behavior is observed for the solutions.⁴ For dilute solutions of side-chain LCPs in LMMNs, $\delta\eta_c$ and $\delta\eta_b$ are usually comparable, which means $R_{\parallel}/R_{\perp} \approx 1$. As a result, eqs 23 and 24 predict that $\delta\alpha_3$ has a positive sign, and $\delta\alpha_2$ has a negative sign which again remains consistent with our experimental observations that a side-chain LCP, dissolved in a flow-aligning LMMN, results in a solution that exhibits flow-tumbling behavior. Since, by definition, the Miesowicz viscosities η_b and η_c are the viscosities when the director is fixed, respectively, in the flow direction and the shear gradient direction, eqs 23 and 24 still satisfy eq 14.

Another important implication of eq 14 is that only three of the four viscosities, α_2 , α_3 , η_b , and η_c , are independent. η_b is known when α_2 , α_3 , and η_c are measurable. Using $\delta\eta_c$ data from earlier ER experiments¹⁶ and $\delta\eta_b$ values obtained, using eq 14, from the

Table 2. Values of $\delta\alpha_2/\delta\alpha_3$ of 5OCB Solutions of the Side-Chain Liquid-Crystalline Polysiloxanes ($T = 62^\circ\text{C}$)

DP	n	modified Brochard model		experimental data		
		R_{\parallel}/R_{\perp}	$\delta\alpha_2/\delta\alpha_3$	$\delta\alpha_2$ (Pa·s)	$\delta\alpha_3$ (Pa·s)	$\delta\alpha_2/\delta\alpha_3$
45	3	1.08 (1.08) ^a	-1.91 ^b	-0.005 84	0.003 13	-1.86
127	3	0.96 (0.96)	-0.69	-0.003 94	0.006 07	-0.65
198	3	0.95 (0.94)	-0.66	-0.005 72	0.008 20	-0.70
45	5	1.17 (1.17)	-3.89	-0.006 93	0.002 18	-3.18
45	11	1.16 (1.18)	-3.58	-0.006 51	0.001 63	-3.99

^a Numbers in parentheses are determined via ER measurements in ref 18. ^b Calculated using the ER values of R_{\parallel}/R_{\perp} from ref 18.

**Figure 11.** DP dependence of $\delta\alpha_2/\delta\alpha_3$ of 5OCB solutions of the side-chain LCPs ($n = 3$, $T = 62^\circ\text{C}$, $c = 0.03\text{ g/mL}$). Experimental data are compared to theoretical predictions using values of R_{\parallel}/R_{\perp} determined from previous ER measurements in ref 18.

numerical analysis of the stress transients shown in Figure 6, R_{\parallel}/R_{\perp} values were calculated via eq 9. The results are listed in Table 2. Good agreement is evident between these results and the values of R_{\parallel}/R_{\perp} reported from earlier ER measurements (shown in parentheses), which were obtained by assuming $\eta_{\text{off}} = \eta_b$ in the previous study.¹⁶

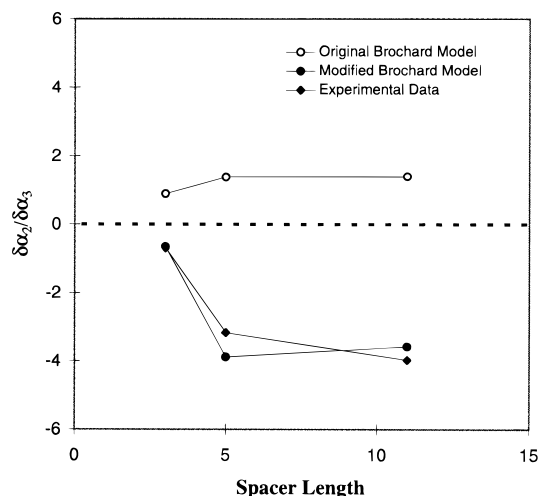
A useful additional result can be obtained by taking the ratio of eqs 23 and 24

$$\delta\alpha_2/\delta\alpha_3 = \left(\frac{1}{2} - \frac{R_{\parallel}^2}{R_{\perp}^2} \right) / \left(\frac{R_{\perp}^2}{R_{\parallel}^2} - \frac{1}{2} \right) \quad (25)$$

which shows that the ratio of the viscosity increments $\delta\alpha_2/\delta\alpha_3$ is solely a function of R_{\parallel}/R_{\perp} . This provides an opportunity to numerically compare experimental values of $\delta\alpha_2/\delta\alpha_3$ (Table 2) determined from the stress transients using Ericksen's TIF theory (eqs 15 and 16) with those calculated from the ER values of R_{\parallel}/R_{\perp} based on the modified Brochard model (eq 25). Such comparisons are tabulated in Table 2 and shown graphically in Figure 11 (for the molecular weight dependence) and Figure 12 (for the spacer length dependence). Taking into account experimental errors, Figures 11 and 12 indicate that the proposed modification of the Brochard theory of the rotational viscosity produces predictions in good agreement with the experimental values from the stress transients via Ericksen's TIF theory.

Conclusions

A systematic study of the stress transients obtained from dilute nematic solutions of a side-chain LCP in a

**Figure 12.** Spacer length dependence of $\delta\alpha_2/\delta\alpha_3$ of 5OCB solutions of the side-chain LCPs ($\text{DP} = 45$, $T = 62^\circ\text{C}$, $c = 0.03\text{ g/mL}$). Experimental data are compared to theoretical predictions using values of R_{\parallel}/R_{\perp} determined from previous ER measurements in ref 18.

flow-aligning nematic solvent has been carried out as a function of LCP concentration, molecular weight, and spacer length. In all cases, the stress transients of the solutions show flow-tumbling behavior, indicative that the increment in the Leslie viscosity coefficient $\delta\alpha_3$ is positive. Analysis of the rheological behavior indicates further that the increment $\delta\alpha_2$ is negative. These results are only partially consistent with the prediction of a molecular hydrodynamic theory by Brochard. Analysis of the discrepancy suggests that an additional contribution to the rotational viscosity is needed. A proposed modification based on the notion that an elastic torque occurs between director rotation and LCP orientation leads to improved agreement with our observations.

Acknowledgment. We gratefully acknowledge the financial support from the National Science Foundation Science and Technology Center ALCOM. We also thank Prof. Shi-Qing Wang for useful discussions.

References and Notes

- (1) de Gennes, P. G.; Prost, J. *The Physics of Liquid Crystals*, 2nd ed.; Clarendon Press: Oxford, U.K., 1993.
- (2) Jamieson, A. M.; Gu, D.-F.; Chen, F.-L.; Smith, S. *Prog. Polym. Sci.* **1996**, *21*, 981.
- (3) Ericksen, J. L. *Arch. Rat. Mech. Anal.* **1960**, *4*, 231.
- (4) Gu, D.; Jamieson, A. M. *Macromolecules* **1994**, *27*, 337.
- (5) Gu, D.; Jamieson, A. M. *J. Rheol.* **1994**, *38*, 555.
- (6) Yang, I.-K.; Shine, A. D. *Macromolecules* **1993**, *26*, 1529.
- (7) Gu, D.; Jamieson, A. M.; Wang, S. Q. *J. Rheol.* **1993**, *37*, 985.
- (8) Han, H. W.; Rey, A. D. *J. Rheol.* **1995**, *39*, 301.
- (9) Han, H. W.; Rey, A. D. *J. Rheol.* **1994**, *38*, 1317.
- (10) Mather, P. T.; Pearson, D. S.; Larson, R. G.; Gu, D.; Jamieson, A. M. *Rheol. Acta*, **1997**, *36*, 485.
- (11) Zuniga, L.; Leslie, F. M. *Europhys. Lett.* **1989**, *9*, 689.
- (12) Burghardt, W. R. Ph.D. Thesis, Stanford University, Stanford, CA, **1990**, Chapter 1.
- (13) Yao, N.; Jamieson, A. M. *J. Rheol.* **1998**, *42*, 603.
- (14) Yao, N.; Jamieson, A. M. Manuscript in preparation.
- (15) Brochard, F. *J. Polym. Sci., Polym. Phys. Ed.* **1979**, *17*, 1367.
- (16) Yao, N.; Jamieson, A. M. *Macromolecules* **1997**, *30*, 5822.
- (17) Gu, D.; Jamieson, A. M.; Rosenblatt, C. M.; Tomazos, D.; Lee, M.; Percec, V. *Macromolecules* **1991**, *24*, 2385.
- (18) Gu, D.; Jamieson, A. M.; Kawasumi, M.; Lee, M.; Percec, V. *Liq. Cryst.* **1992**, *12*, 961.
- (19) Gu, D.; Smith, S. R.; Jamieson, A. M.; Lee, M.; Percec, V. *J. Phys. II Fr.* **1993**, *12*, 961.
- (20) Chen, F.-L.; Jamieson, A. M. *Macromolecules* **1993**, *26*, 6576.

- (21) Chiang, Y.-C.; Jamieson, A. M.; Kawasumi, M.; Percec, V. *Macromolecules* **1997**, *30*, 1992.
- (22) Jamieson, A. M.; Chiang, Y.-C.; Smith, S. R. *Macromol. Symp.* **1997**, *118*, 289.
- (23) Chiang, Y.-C.; Jamieson, A. M.; Campbell, S.; Lin, Y.; O'Sidocky, N.; Chien, L. C.; Kawasumi, M.; Percec, V. *Acta Rheol.* **1997**, *36*, 505.
- (24) Parodi, O. *J. Phys.* **1970**, *31*, 581.
- (25) Marrucci, G. *Pure Appl. Chem.* **1985**, *57*, 1545.
- (26) Williams, D. R. M.; Halperin, A. *Macromolecules* **1993**, *26*, 2025.

MA980143U